

# Measuring black-hole parameters and testing general relativity using gravitational-wave data from space-based interferometers

Eric Poisson\*

*Department of Physics, University of Guelph, Guelph, Ontario, N1G 2W1, Canada<sup>†</sup>;  
McDonnell Center for the Space Sciences, Department of Physics, Washington University, St. Louis, Missouri, 63130  
(Submitted to Physical Review D, June 12, 1996)*

Among the expected sources of gravitational waves for the Laser Interferometer Space Antenna (LISA) is the capture of solar-mass compact stars by massive black holes residing in galactic centers. We construct a simple model for such a capture, in which the compact star moves freely on a circular orbit in the equatorial plane of the massive black hole. We consider the gravitational waves emitted during the late stages of orbital evolution, shortly before the orbiting mass reaches the innermost stable circular orbit. We construct a simple model for the gravitational-wave signal, in which the phasing of the waves plays the dominant role. The signal's behavior depends on a number of parameters, including  $\mu$ , the mass of the orbiting star,  $M$ , the mass of the central black hole, and  $J$ , the black hole's angular momentum. We calculate, using our simplified model, and in the limit of large signal-to-noise ratio, the accuracy with which these quantities can be estimated during a gravitational-wave measurement. For concreteness we consider a typical system consisting of a  $10 M_{\odot}$  black hole orbiting a nonrotating black hole of mass  $10^6 M_{\odot}$ , whose gravitational waves are monitored during an entire year before the orbiting mass reaches the innermost stable circular orbit. Defining  $\chi \equiv cJ/GM^2$  and  $\eta \equiv \mu/M$ , we find  $\Delta\chi \simeq 5 \times 10^{-2}/\rho$ ,  $\Delta\eta/\eta \simeq 6 \times 10^{-2}/\rho$ , and  $\Delta M/M \simeq 2 \times 10^{-3}/\rho$ . Here,  $\rho$  denotes the signal-to-noise ratio associated with the signal and its measurement. That these uncertainties are all much smaller than  $1/\rho$ , the signal-to-noise ratio level, is due to the large number of wave cycles received by the detector in the course of one year. These are the main results of this paper. Our simplified model also suggests a method for experimentally testing the strong-field predictions of general relativity.

Pacs Numbers: 04.30.-w; 04.30.Db; 04.70.-s; 04.80.Cc; 95.55.Ym; 97.60.L

## I. INTRODUCTION AND SUMMARY

### A. Space-based gravitational-wave detectors

The Laser Interferometer Space Antenna (LISA) project [1] was proposed in December 1993 as a cornerstone project for the "Horizon 2000 Plus" program of the European Space Agency. If the project is realized, LISA might start searching for gravitational waves in the year 2010.

The LISA interferometer consists of three pairs of spacecrafts, each pair located at the corners of an equilateral triangle. The constellation moves on a heliocentric orbit at 1 AU, following the Earth by an angle of  $20^\circ$ . Each side of the triangle has a length of  $5 \times 10^6$  km, and the plane of the triangle is oriented at  $60^\circ$  with respect to the ecliptic.

LISA uses laser interferometry to detect gravitational waves in the frequency band between 0.1 and 100 mHz. Such waves have much too low a frequency to be measurable by Earth-based interferometers, which are severely limited by seismic noise at these frequencies [2]. LISA's projected sensitivity is such that a gravitational wave of amplitude  $10^{-23}$  would give rise to a signal-to-noise ratio of 5 after one year of observation.

Among the expected sources of gravitational waves relevant to LISA are solar oscillations [3], binary systems of normal and compact stars within the galaxy [4], massive black-hole binaries in other galaxies [1], and primordial gravitational waves [5].

In this paper we consider another type of source, also expected to be highly relevant: the capture of solar-mass compact stars by massive black holes [6,7].

### B. Stellar capture by massive black holes

The most likely explanation for active galactic nuclei involves the tidal disruption of normal stars by a massive black hole residing in the galactic center. It is plausible that compact stars (such as neutron stars and black holes) will also be captured by the massive black hole. However, such stars will not be disrupted, and their complex orbital motion will generate gravitational waves [6]. If the central black hole has a mass in the interval between  $10^5$  and  $10^7$  solar masses, then these waves will have their frequency within the LISA bandwidth [1], and will be detected if they are sufficiently strong.

It is expected that typically, a captured star will move on a highly eccentric orbit around the massive black hole [6–9]. Such orbits are easily perturbed by the other stars

in the galactic nucleus, and this can have a damaging effect on the gravitational-wave signal. The probability for an orbit to be perturbed decreases with increasing values of the orbiting mass. For this reason it is judged [1,10] that the capture of compact stars with masses in the interval between 5 and 10 solar masses would be the most relevant for observations by LISA. Compact stars of such masses cannot be neutron stars, and would therefore be black holes. It was estimated [1,10] that the rate of occurrence for such events could be as large as several per year, and that the signal-to-noise ratio could be near 40 for a capture occurring at a distance corresponding to a cosmological redshift of one.

In this paper we consider the gravitational waves produced during the capture of a  $10 M_{\odot}$  black hole by a massive,  $10^6 M_{\odot}$  black hole. We are specifically interested in what can be learned from observing these waves.

### C. Information carried by the waves

The gravitational waves produced during the capture of a compact star by a massive black hole are rich in information. In principle, measuring the waves should allow us to extract the value of the black-hole parameters (mass and angular momentum), as well as to test the strong-field predictions of general relativity [11]. In this paper we wish to propose a strategy for doing both.

A possible method for extracting the black-hole parameters, which we shall not explore in this paper, would go as follows [12].

The gravitational waves generated by the bound motion of a mass around a center come with a certain distribution in frequency. For example, circular motion in the equatorial plane of a black hole produces waves with frequencies at every harmonic of the orbital frequency [13]. (The strongest waves come at twice the orbital frequency.) As an other example, the gravitational waves produced by a mass in eccentric motion (also in the equatorial plane) come in harmonics of two fundamental frequencies [7,9,8], respectively associated with the angular and radial components of the motion.

Precisely how the waves are distributed in frequency depends on the orbital parameters (for example, the eccentricity). Measuring the distribution at some moment in time therefore leads to an estimation of these parameters. Now, because the system is losing energy and angular momentum to gravitational waves, the orbital parameters are not constant, but evolve in time. Precisely how they do so depends on the black-hole parameters (and also on the mass of the orbiting object). Measuring how the orbital parameters evolve in time therefore leads to an estimation of the black-hole parameters.

Such a method was recently examined by Finn, Ori, and Thorne [12], in the restricted context of circular, equatorial orbits. The method involves measuring the relative amplitude of each frequency component of the

gravitational waves. In Sec. V we will see that amplitude measurements typically come with relative statistical uncertainties of order  $1/\rho$ , where  $\rho$  is the signal-to-noise ratio associated with the signal and its measurement. (The uncertainty is due to the detector noise.) It follows that by using this method, the estimation of the black-hole parameters can be effected with a relative accuracy of order  $1/\rho$ .

Another method for extracting the black-hole parameters, also not explored in this paper, would involve monitoring that part of the gravitational-wave signal which corresponds to the black hole settling down after the orbiting mass' final plunge [14,15]. This part of the signal is strongly dominated by the black-hole quasi-normal modes [16], whose frequencies and damping times are functions of the hole's mass and angular momentum. Such a method was examined by Echeverria [14] and Finn [15], who also conclude that the black-hole parameters can be estimated with a relative accuracy of order  $1/\rho$ .

The method considered in this paper is essentially due to Finn and Chernoff [17], and to Cutler and Flanagan [18]. It goes as follows.

As was pointed out above, the gravitational waves come in many frequency components. One of these, preferably the dominant one, is selected, and its phase is carefully monitored. Let us denote by  $f$  the frequency of this component. Because the system loses energy and angular momentum to gravitational waves,  $f$  increases slowly with time. The phasing of the waves is determined by  $df/dt$ , the rate of change of the frequency. In turn, this depends on the black-hole parameters (and also on the mass of the orbiting object). Monitoring the phase therefore leads to a way of estimating the black-hole parameters.

We will show in Sec. V that the estimation of those parameters which influence the phasing of the waves can be effected with a relative accuracy of order  $1/\rho_{\text{eff}}$ , where the *effective* signal-to-noise ratio is given by  $\rho_{\text{eff}} = 2\pi\mathcal{N}\rho$ . Here,  $\mathcal{N}$  is the total number of wave cycles received by the gravitational-wave detector. This number will be estimated in Sec. III: For a binary system consisting of two black holes, one of mass  $10 M_{\odot}$ , the other of mass  $10^6 M_{\odot}$ , and for a signal monitored during an entire year,  $\mathcal{N} \simeq 10^5$ . The method considered in this paper therefore leads to a much enhanced accuracy for the estimation of the black-hole parameters.

### D. Realistic captures and our simplified model

The realistic description of a capture is complicated. The captured star moves on a highly eccentric orbit [6–9] which may not lie in the equatorial plane of the massive black hole. The orbital parameters (such as periastron and eccentricity) evolve in time, in part stochastically (due to perturbation by other stars) and in part secularly (due to gravitational radiation reaction).

To model a realistic capture, and to calculate the gravitational waves emitted, is a difficult problem. To a first approximation, in which one ignores the external perturbation and the radiation reaction, the orbit is accurately represented by a bound geodesic of the Kerr spacetime [19,20]. Such an orbit is characterized by three parameters: orbital energy, orbital angular momentum, and a third called the Carter constant.

An improved approximation would incorporate a small stochastic variation of these parameters, which would account for the external perturbation, and also a small secular variation, which would account for the radiation reaction [7–9]. This approximation should be quite accurate if the density of stars is sufficiently low near the central black hole.

The main difficulty preventing this problem from finding a solution resides in the fact that no prescription is currently available for calculating the secular evolution of the Carter constant. (See, however, Refs. [21–23]. The evolution of the other orbital parameters is obtained by computing how much energy and angular momentum are carried off by the gravitational waves. This is done by applying the methods of black-hole perturbation theory [7–9].) However, because of the system’s small mass ratio, this problem should be much more tractable than the nonrestricted general relativistic two-body problem, which currently is only amenable to post-Newtonian methods [24].

In this paper we choose to simplify the problem as much as possible, in order to introduce a simple, analytic expression for the gravitational-wave signal. We shall assume that the captured object moves freely on a circular orbit in the equatorial plane of the massive black hole. We shall ignore all external perturbations, and focus on the secular evolution induced by the emission of gravitational waves. Because the orbit is circular and equatorial, this evolution is dictated entirely by the loss of orbital energy. And because the ratio of the two masses is small, this loss is accurately computed using the methods of black-hole perturbation theory [25].

### E. Model gravitational-wave signal

As the system loses energy and angular momentum to gravitational waves,  $f$ , the frequency of the selected gravitational-wave component, slowly increases. For a circular orbit, the dominant component is at twice the orbital frequency; if  $\Omega$  denotes the angular velocity of the orbiting mass, then  $2\pi f = 2\Omega$ . It can be shown [9] that during most of the orbital evolution, the *adiabatic approximation* holds. This states that the radiation reaction timescale is much longer than the orbital period, so that  $df/dt \ll 1/f^2$ . Our analysis relies heavily on the adiabatic approximation.

There exists an upper bound for the gravitational-wave frequency, which we denote by  $f_0$ . This bound is set by

the innermost stable circular orbit (ISCO) of the Kerr spacetime, and is equal to  $\Omega_0/\pi$ , where  $\Omega_0$  is the angular velocity of a test mass moving on the ISCO. The gravitational waves therefore sweep up in frequency until  $f = f_0$ . At this point, the orbiting mass can no longer maintain a circular orbit, and is forced to plunge into the massive black hole, thereby shutting off the gravitational waves. It should be noted that the adiabatic approximation necessarily breaks down as the orbiting mass reaches the ISCO [9].

We shall focus our attention on that part of the orbital evolution for which the gravitational waves are strongest and most interesting. This corresponds to the very late stages, shortly before the orbiting mass reaches the ISCO. If we assume that  $f$  is always very close to  $f_0$ , then we may express all relevant quantities as Taylor expansions about the ISCO.

We are mostly interested in the phasing of the waves, which is determined by  $df/dt$ . We will find in Sec. II B that this can be expressed as

$$\frac{df}{dt} = \frac{\pi}{3} \frac{\mathcal{V}f_0^2}{1 - f/f_0} \left[ 1 - 2\alpha(1 - f/f_0) + \dots \right]. \quad (1.1)$$

Here,  $\mathcal{V}$  and  $\alpha$  are dimensionless expansion coefficients which depend on  $\mu$ , the mass of the orbiting star,  $M$ , the mass of the central black hole, and  $|\chi| \equiv J/M^2$ , its dimensionless angular-momentum parameter. (We use units such that  $G = c = 1$ ;  $J$  denotes the black hole’s spin angular momentum, and  $\chi$  will be defined more precisely in Sec. IV.) The dots denote terms of higher order in  $1 - f/f_0$ . It is to be noted that Eq. (1.1) is singular at  $f = f_0$ . This reflects the breakdown of the adiabatic approximation at the ISCO. This issue is discussed in detail in Sec. II C.

We use Eq. (1.1) to construct a model for the gravitational-wave signal originating from the capture of a compact star by a massive black hole. The model signal then depends on the parameters  $f_0$ ,  $\mathcal{V}$ , and  $\alpha$ , which codify information about the source. We ask how well these parameters can be estimated during a gravitational-wave measurement, and what they can tell us about  $\mu$ ,  $M$ , and  $\chi$ .

In the following we will refer to  $\{f_0, \mathcal{V}, \alpha\}$  as the *signal* parameters, and to  $\{\mu, M, \chi\}$  as the *source* parameters.

### F. A remark on our expansion approach

The expansion (1.1) is accurate only if  $1 - f/f_0$  is always much smaller than unity. We must ask whether this is true for a system with  $\mu = 10 M_\odot$ ,  $M = 10^6 M_\odot$ , whose gravitational waves are monitored for an entire year before the orbiting mass reaches the innermost stable circular orbit. The answer, most unfortunately, is no. For such a system, as we shall see in Sec. III,  $\varepsilon \equiv \Delta f/f_0 \simeq 1.1$ , where  $\Delta f$  is the frequency interval over which the signal is monitored.

To build a model signal upon such expansions as Eq. (1.1) therefore seems a bad idea if one is at all interested in accuracy. Should we then give up this approach and do something better? We choose to give a negative answer: We will not give up, and we shall proceed with our expansions, even though the resulting signal may not be very accurate.

The reason is that to provide a better representation for  $df/dt$  would require a great deal more work, and could not be done in the simple, analytic way advocated in this paper. Indeed, the gravitational-wave signal would have to be generated numerically. Now, numerical signals *will* have to be provided when an attempt is made to construct more sophisticated models, for example, models that incorporate highly eccentric orbits. However, we feel it would not be worthwhile to introduce numerical signals at this stage.

Instead, for the sake of simplicity, we shall continue to treat  $1 - f/f_0$  as a formally small quantity, and to carry out expansions in powers of that quantity. We hope that our conclusions will not depend strongly on this assumption, and that we can safely put  $\varepsilon \simeq 1$  at the end of the calculation.

### G. The main results

Our model gravitational-wave signal is characterized by the parameters  $f_0$ ,  $\mathcal{V}$ , and  $\alpha$ , which are functions of the source parameters  $\mu$ ,  $M$ , and  $\chi$ .

The signal parameters can be estimated during a gravitational-wave measurement. The statistical uncertainties associated with such an estimation are calculated in detail in Sec. V, in the limit of large signal-to-noise ratio. For concreteness we consider a typical system consisting of a  $10 M_\odot$  black hole orbiting a nonrotating black hole of mass  $10^6 M_\odot$ , whose gravitational waves are monitored for an entire year before the orbiting mass reaches the innermost stable circular orbit. For such a system we find that the measurement uncertainties are given by

$$\begin{aligned} \frac{\Delta f_0}{f_0} &\simeq 5.5 \times 10^{-4}/\rho, \\ \frac{\Delta \mathcal{V}}{\mathcal{V}} &\simeq 3.8 \times 10^{-3}/\rho, \\ \Delta \alpha &\simeq 1.0 \times 10^{-2}/\rho, \end{aligned} \quad (1.2)$$

where  $\rho$  is the signal-to-noise ratio. A more precise, and more general, statement of these results appears in Eq. (5.12). These uncertainties should be compared with that associated with  $\mathcal{A}$ , the signal's amplitude parameter:  $\Delta \mathcal{A}/\mathcal{A} = 1/\rho$ . That the phase parameters can be estimated much more accurately is due to the large number of wave cycles received by the detector. We indeed recall that  $\mathcal{N} \sim 10^5$ .

Equations (1.2) imply that the source parameters  $\chi$ ,  $\eta \equiv \mu/M$ , and  $M$  can be determined with uncertainties

$$\begin{aligned} \Delta \chi &\simeq 5.0 \times 10^{-2}/\rho, \\ \frac{\Delta \eta}{\eta} &\simeq 5.5 \times 10^{-2}/\rho, \\ \frac{\Delta M}{M} &\simeq 2.4 \times 10^{-3}/\rho. \end{aligned} \quad (1.3)$$

A more precise, and more general, statement of these results can be found in Sec. V C. We recall from Sec. I B that gravitational waves produced during a capture occurring at cosmological distances could be measured with  $\rho \simeq 40$ .

### H. Testing general relativity

In order to obtain Eqs. (1.3) from (1.2), the relation between the source parameters  $\{\mu, M, \chi\}$  and the signal parameters  $\{f_0, \mathcal{V}, \alpha\}$  must be known. This relation is based upon two conditions: that the central mass is a Kerr black hole, and that the system emits gravitational waves according to the quantitative predictions of Einstein's theory. Indeed, general relativity is used to calculate  $dE/dt$ , the energy lost per unit time to gravitational waves. It is also used to write  $f = \Omega/\pi$ , the statement that the strongest waves come at twice the orbital frequency. On the other hand, the Kerr metric is used to calculate  $dE/d\Omega$ , the relation between orbital energy and angular velocity. Putting all this together gives  $df/dt$  in terms of the source parameters.

It is easy to imagine a situation in which either one, or both, of these conditions would be violated. For example, the central mass could be something quite different from a Kerr black hole, or Einstein's theory could make wrong predictions regarding the emission of gravitational waves. As a specific example, we may recall that in the Brans-Dicke theory [26], the existence of scalar radiation implies a different result for  $dE/dt$  from what is predicted by general relativity [27]. However, by virtue of the uniqueness of the Kerr black hole [28], the relation  $dE/d\Omega$  is preserved in the Brans-Dicke theory.

A breakdown of what we shall call the standard model (general relativity is valid and the central mass is a Kerr black hole) does not logically invalidate Eq. (1.1). Indeed, this equation is based solely on the assumptions that the orbiting mass moves on a circular orbit, and that the spacetime possesses an innermost stable circular orbit. These conditions could easily be preserved in an alternative model.

The standard model implies a particular relationship between the source and signal parameters. Another model would presumably imply a different relationship. We may therefore ask whether a measurement of the signal parameters might allow us to test the validity of the standard model. This question is considered in Sec. V D, where we show that a measurement of  $\alpha$  outside the interval  $(-\infty, 1.8)$  would unambiguously signal the breakdown of the standard model.

## I. Conclusion

The analysis presented in this paper is by no means definitive, and needs to be improved in many respects. First, the crude representation (1.1) for  $df/dt$  will have to be replaced by something more reliable, presumably of numerical form. Second, the unrealistic assumption that the orbit must be equatorial and circular will have to be removed. All of this will require a great deal of effort.

However, our simplified analysis should not be criticized too harshly. It is, after all, a first approach to a difficult problem. And our conclusions show promise: We believe that our results (1.3) for the measurement accuracies — most especially the fact that the phasing method yields uncertainties which are much smaller than  $1/\rho$  — provide ample motivation for pursuing this work and adding new layers of complexity.

## J. Organization of this paper

We begin in Sec. II with a detailed introduction of our model for the gravitational-wave signal. The assumptions are reviewed and explained in Sec. II A. The signal is explicitly constructed in Sec. II B. Finally, some of the approximations employed are motivated in Sec. II C.

In Sec. III we consider a specific case of the general framework introduced in Sec. II, in which the central mass is a Schwarzschild black hole. This section also provides numerical estimates for such quantities as  $f_0$ ,  $\mathcal{V}$ ,  $\alpha$ ,  $\varepsilon$ , and  $\mathcal{N}$ .

In Sec. IV we generalize the discussion of Sec. III to the case of a Kerr black hole.

Section V contains a discussion of the statistical uncertainties associated with the estimation of the signal parameters. In Sec. V A we re-introduce the model signal. In Sec. V B, expressions are derived for the measurement uncertainties. These are converted, in Sec. V C, into uncertainties for the source parameters, assuming the validity of the standard model. Finally, in Sec. V D, a method is proposed to test the validity of the standard model.

The Appendix contains a general discussion of orbital motion in spacetimes which are stationary, asymptotically flat, axially symmetric, and reflection symmetric about the equatorial plane. (The orbits are restricted to this plane.) The equations of motion are introduced in Sec. A 1. Circular orbits are defined precisely in Sec. A 2. In Sec. A 3 we consider two neighboring circular orbits, and derive relationships between the displacements in radius, energy, angular momentum, and angular velocity. Finally, the innermost stable circular orbit is defined precisely in Sec. A 4.

## II. MODEL GRAVITATIONAL-WAVE SIGNAL

In this section we introduce our model for the gravitational waves emitted during the late stages of orbital evolution of a binary system with small mass ratio, shortly before the smaller mass reaches the innermost stable circular orbit associated with the larger mass. In Sec. II A we list and explain the assumptions involved in formulating the model. In Sec. II B we construct the signal. In Sec. II C we discuss the validity of some of the approximations used in subsection B.

### A. Assumptions

To formulate the model we shall make a number of assumptions. These are listed and explained below.

*Assumption 1:* The binary system consists of a small mass  $\mu$  and a large mass  $M$ , so that  $\mu/M \ll 1$ . In typical situations we shall take  $\mu = 10 M_\odot$  and  $M = 10^6 M_\odot$ .

*Assumption 2:* The spacetime geometry associated with the mass  $M$  is stationary, asymptotically flat, axially symmetric, and reflection symmetric about the equatorial plane. However, it is not assumed that  $M$  is a Kerr black hole, or even that the metric is a solution to the Einstein field equations. Although most of this paper will be devoted to the specific case of a Kerr black hole, we wish to keep the framework as general as possible in order to later identify a strategy for experimentally testing the predictions of general relativity.

Assumption 2 leads to a number of simplifications. First, the fact that the spacetime is stationary and axially symmetric implies that  $\Omega = d\phi/dt$ , the angular velocity of the orbiting mass  $\mu$ , is uniform if the orbit is circular. Here,  $\phi$  is the angle that goes around the axis of symmetry, and  $t$  is proper time for observers at rest at infinity. Second, the fact that the spacetime is reflection symmetric about the equatorial plane implies that if started in this plane, the orbit will remain in the plane forever (whether it is circular or not). Consequently, we can further impose:

*Assumption 3:* The mass  $\mu$  moves on a circular orbit in the equatorial plane of the mass  $M$ . This assumption is imposed solely for the sake of simplicity, and cannot be expected to hold in realistic situations. This was discussed in detail in Sec. I D.

*Assumption 4:* The spacetime possesses an innermost stable circular orbit (ISCO). The ISCO is defined to be that particular circular orbit for which an infinitesimal change in orbital energy induces a large change in the orbital radius, or in the angular velocity  $\Omega$ .

The ISCO can be thought of as the limiting member of a sequence of circular orbits, each labeled by the value of its angular velocity. For  $\Omega$  smaller than the critical value  $\Omega_0$ , stable circular orbits exist; for  $\Omega$  larger than  $\Omega_0$ , circular orbits are no longer mechanically stable. Bound orbits within the ISCO all plunge toward the mass  $M$ .

*Assumption 5:* The binary system emits gravitational waves. It is not assumed that Einstein's theory gives the correct description of gravitational radiation, for the same reason as was expressed in the context of assumption 2.

Due to the emission of gravitational waves, the system loses energy and angular momentum, and as a result, the mass  $\mu$  undergoes orbital evolution: its angular velocity does not stay constant but keeps on increasing as the orbital radius decreases.

Combining assumptions 1 and 5 leads to the consequence that while  $\Omega$  increases due to the radiation reaction, this increase occurs *adiabatically* [9]: the timescale for the increase is much larger than the orbital period. The orbital evolution can therefore be represented by a succession of circular orbits (ordered by the increasing value of the angular velocity), with the mass  $\mu$  moving quasi-statically from one orbit to the next.

It is important to state that the adiabatic approximation must break down as the orbiting mass reaches the innermost stable circular orbit [9]. This follows from the very definition of the ISCO. Nevertheless, the adiabatic approximation holds for most of the orbital evolution, and its breakdown will not be an obstacle in the forthcoming analysis.

*Assumption 6:* The gravitational waves emitted by the binary system are monitored by a space-based interferometric detector (such as LISA) during an entire year before the mass  $\mu$  reaches the innermost stable circular orbit.

We shall calculate that during this time, the angular velocity changes by a fractional amount of order unity. We shall also find that  $\mathcal{N}$ , the total number of wave cycles received by the detector during the year's worth of observation, is quite large. In typical situations,  $\mathcal{N} \sim 10^5$ .

## B. Construction of the signal

In brief, the model gravitational-wave signal is based upon a Taylor expansion about the innermost stable circular orbit. The justification for this was given in Sec. I F, and will be repeated in Sec. II C. The model signal is also based upon the adiabatic approximation, which is itself a consequence of assumptions 1 and 5. And finally, we shall construct the signal by focusing mostly on its *phasing*, as was motivated in Sec. I C.

We now proceed. Combining the adiabatic approximation with assumption 3 (regarding the circularity of the orbit) implies that the gravitational waves have a frequency component at *every* harmonic of the angular velocity  $\Omega(t)$ . (Here we indicate that the angular velocity evolves slowly with time.) More precisely [9,13], the frequency  $F_m$  associated with the  $m$ 'th harmonic is given by  $2\pi F_m(t) = m\Omega(t)$ . We single out the strongest frequency component, and assume that only this component is actually measured by the gravitational-wave detector. (In

general relativity the dominant harmonic is at  $m = 2$ .) This particular frequency will be denoted by  $F(t)$ .

The phasing of the wave is determined by the function  $F(t)$ . To obtain this we invoke once again the adiabatic approximation, and write

$$\frac{dF}{dt} = \frac{dE/dt}{dE/dF}, \quad (2.1)$$

where  $E$  denotes the orbital energy of the mass  $\mu$ . The numerator of Eq. (2.1) represents the energy lost per unit time to gravitational waves. The denominator gives the relationship between orbital energy and angular velocity. The adiabatic approximation ensures that  $E$  and  $F$  change very little over the course of one orbit, so that these quantities are actually well defined. As was pointed out before, the adiabatic approximation, and therefore Eq. (2.1) also, break down as the mass  $\mu$  reaches the innermost stable circular orbit. This does not represent an obstacle to our modeling; we will return to this point in Sec. II C.

We denote by  $f_0$  the gravitational-wave frequency at the innermost stable circular orbit. To indicate that  $f_0$  must scale as the inverse power of  $M$ , we introduce the notation

$$\pi M f_0 \equiv v_0^3, \quad (2.2)$$

where  $v_0$  is a scale-invariant quantity; the factor of  $\pi$  was inserted for convenience.

We expand  $dE/dt$  about the innermost stable circular orbit. Since the gravitational-wave luminosity must scale as the square of the mass ratio, we write

$$\frac{dE}{dt} = -\left(\frac{\mu}{M}\right)^2 v_0^{10} p [1 - \hat{p}(1 - F/f_0) + \dots]. \quad (2.3)$$

Here,  $p$  and  $\hat{p}$  are phenomenological parameters. The value that these parameters take depends on the nature of the mass  $M$  and on the correct description of gravitational radiation. Specific cases will be considered in Sec. III and VI. For the time being, however, we leave these parameters undetermined. The factor of  $v_0^{10}$  was inserted for convenience, and the dots designate terms of higher order in  $1 - F/f_0$ .

We also expand  $dE/dF$  about the innermost stable circular orbit. To do this we recall that the ISCO is defined to be that particular orbit for which an infinitesimal change in orbital energy produces a large change in the orbital radius, or in the angular velocity (which is related to the radius by a Kepler-type relation). The defining property of the ISCO is therefore that  $dE/dF$  must go to zero there. (See the Appendix for further details, and for a justification of the fact that  $dE/dF$  must vanish linearly with  $1 - F/f_0$ .) We also note that  $dE/dF$  must scale like the product of the two masses, as can be quickly seen from an elementary Newtonian calculation. We therefore write

$$\frac{dE}{dF} = -\frac{\mu M}{v_0} q (1 - F/f_0) [1 - \hat{q}(1 - F/f_0) + \dots]. \quad (2.4)$$

As before,  $q$  and  $\hat{q}$  are phenomenological parameters, and a factor of  $1/v_0$  was inserted for convenience.

Combining Eqs. (2.1)–(2.4) yields

$$\frac{dF}{dt} = \frac{\pi}{3} \mathcal{V} f_0^2 (1 - F/f_0)^{-1} [1 - 2\alpha (1 - F/f_0) + \dots], \quad (2.5)$$

where

$$\mathcal{V} = \frac{3\pi p}{q} \frac{\mu}{M} v_0^5, \quad \alpha = \frac{1}{2}(\hat{p} - \hat{q}). \quad (2.6)$$

Equation (2.5) can easily be integrated to give  $t(F)$ , and the phase function

$$\Phi(F) = \int 2\pi F(t) dt = \int 2\pi F \frac{dt}{dF} dF \quad (2.7)$$

can be obtained similarly.

We take the time-domain gravitational-wave signal to be

$$h(F(t)) = \mathcal{A}(1 + \dots) e^{-i\Phi(F)}. \quad (2.8)$$

Here,  $\mathcal{A}$  is the signal's amplitude at the time the mass  $\mu$  reaches the innermost stable circular orbit;  $\mathcal{A}$  is inversely proportional to the distance to the source. We shall also need an expression for the frequency-domain signal, which is obtained by Fourier transforming  $h(t)$ :

$$\tilde{h}(f) = \int h(t) e^{2\pi i f t} dt = \int h(F) e^{2\pi i f t(F)} \frac{dt}{dF} dF. \quad (2.9)$$

The frequency  $f$  must be distinguished from  $F(t)$ , the function of time which was also referred to as the frequency.

We evaluate the Fourier transform by invoking the stationary-phase approximation [29], which actually follows from the adiabatic approximation [18]. (We shall return to this point shortly.) After substituting Eq. (2.8) into (2.9), we find that the argument of the exponential becomes  $i$  times  $2\pi f t(F) - \Phi(F) \equiv \varphi(F)$ . Using Eq. (2.7), we see that this phase has a stationary point when  $0 = d\varphi/dF = 2\pi(f - F)(dt/dF)$ , that is, when  $F = f$ . The stationary-phase approximation then returns a factor  $[-\varphi''(f)]^{-1/2} \propto (1 - f/f_0)^{-1/2}$  which must be combined with the factor  $dt/dF|_f \propto (1 - f/f_0)$  coming from inside the integral. After simple manipulations, including the absorption of constants into a redefinition of  $\mathcal{A}$ , we arrive at

$$\begin{aligned} \tilde{h}(f) &= \mathcal{A}(1 + \dots) (1 - f/f_0)^{1/2} e^{i\psi(f)}, \\ \psi(f) &= 2\pi f t_0 - \phi_0 + \phi(f), \\ \phi(f) &= \frac{(1 - f/f_0)^3}{\mathcal{V}} [1 + \alpha(1 - f/f_0) + \dots]. \end{aligned} \quad (2.10)$$

Here, the constants  $t_0 \equiv t(f_0)$  and  $\phi_0 \equiv \Phi(f_0) + \pi/4$  respectively represent time and phase at the innermost

stable circular orbit. As before, the dots designate terms of higher order in  $1 - f/f_0$ .

We shall adopt Eq. (2.10) as our model for the (frequency-domain) gravitational-wave signal. It involves six phenomenological parameters: the amplitude  $\mathcal{A}$ , the final time  $t_0$ , the final phase  $\phi_0$ , the final frequency  $f_0$ , as well as  $\mathcal{V}$  and  $\alpha$  coming from the expansion of  $dF/dt$  about the innermost stable circular orbit.

### C. Validity of approximations

Our model gravitational-wave signal is based upon a Taylor expansion about the innermost stable circular orbit. Such an expansion can be accurate only if  $1 - f/f_0$  is small throughout the entire frequency interval over which the signal is monitored. If  $f_i$  denotes the initial value of the frequency, we would require  $\varepsilon \equiv 1 - f_i/f_0 \ll 1$ .

In Sec. III we will find that in typical situations,  $\varepsilon \simeq 1.1$ , and is therefore not small. This means that our model signal cannot be very accurate for frequencies near  $f_i$ . This is most unfortunate, but we shall nevertheless proceed with our model signal, which at least has the virtue of being extremely simple. In view of the fact that our model also incorporates unrealistic assumptions (that the orbit must be equatorial and circular), we feel that this degree of sophistication should be sufficient for our purposes. We do not expect that the use, in our calculations, of a more exact representation for  $dF/dt$  would lead to very different conclusions. A more complete discussion of this point was given in Sec. I F.

We now discuss the breakdown of the adiabatic and stationary-phase approximations. The adiabatic approximation becomes invalid when the timescale over which  $F(t)$  changes becomes comparable to the orbital period. This translates to  $(1/F)(dF/dt) \sim F$  or, upon using Eq. (2.5) and  $F \sim f_0$ ,

$$(1 - F/f_0) \sim \mathcal{V}. \quad (2.11)$$

It can be shown that the same criterion applies to the breakdown of the stationary-phase approximation [18].

To circumvent the problems associated with the breakdown of these approximations, we shall impose that Eq. (2.10) is valid for

$$f < f_f \equiv f_0 (1 - \mathcal{V}) \quad (2.12)$$

only. For  $f > f_f$ , the signal is taken to be identically zero. In any event, the part of the signal for which Eq. (2.12) is violated turns out to be irrelevant for the purpose of Sec. V. Indeed, we shall see that most of the signal-to-noise ratio is accumulated when  $(1 - f/f_0)$  is much larger than  $\mathcal{V}$ . This is reflected in Eq. (5.4), below.

### III. SCHWARZSCHILD BLACK HOLE

To give concreteness to the framework introduced in the preceding section, and to prepare the way for the next, here we consider the special case in which the mass  $M$  is a Schwarzschild black hole. In this and the following section we assume that general relativity gives the correct description of gravitational radiation.

In this context, the signal's dominant frequency is at twice the orbital frequency, so that  $2\pi F = 2\Omega = 2(M/r^3)^{1/2}$ , where  $r$  is the orbital radius in Schwarzschild coordinates. Since the innermost stable circular orbit is located at  $r = 6M$  [19], Eq. (2.2) gives

$$v_0 = 6^{-1/2} \simeq 0.4083. \quad (3.1)$$

The gravitational waves emitted by a mass  $\mu$  in circular motion near the ISCO of a Schwarzschild black hole of mass  $M$  can be calculated using the methods of black-hole perturbation theory [13,30,31]. The numerical evaluation of  $dE/dt$  then yields estimates for the constants  $p$  and  $\hat{p}$  appearing in Eq. (2.3). Using the results presented in Ref. [32], we obtain

$$p \simeq 7.30, \quad \hat{p} \simeq 3.78. \quad (3.2)$$

On the other hand,  $dE/dF$  can be calculated analytically, since this quantity relates orbital energy and angular velocity for circular geodesics of the Schwarzschild spacetime. An elementary calculation yields

$$E = \mu(1 - 2v^2)(1 - 3v^2)^{-1/2}, \quad (3.3)$$

where  $v = (M/r)^{1/2} = (M\Omega)^{1/3} = (\pi MF)^{1/3}$ . After differentiation,

$$\frac{dE}{dF} = -\frac{\pi\mu M}{3v} (1 - 6v^2)(1 - 3v^2)^{-3/2}. \quad (3.4)$$

Finally, expansion about  $F = f_0 = (6^{3/2}\pi M)^{-1}$  yields Eq. (2.4), with

$$q = \frac{4\sqrt{2}\pi}{9} \simeq 1.9746, \quad \hat{q} = \frac{1}{2}. \quad (3.5)$$

We now use the results obtained thus far to estimate the parameters which characterize the gravitational-wave signal.

We begin with the final-frequency parameter,  $f_0$ . Use of Eqs. (2.2) and (3.1) yields the relationship between  $f_0$  and  $M$ , which we write as

$$f_0 = 4.40 \left( \frac{v_0}{0.4083} \right)^3 \left( \frac{M}{10^6 M_\odot} \right)^{-1} \text{ mHz}. \quad (3.6)$$

We have chosen a fiducial value of  $1 \times 10^6 M_\odot$  for  $M$ , to ensure that for such a mass,  $f_0 = 4.4 \times 10^{-3}$  Hz, where LISA's sensitivity is near maximum. In the way it is written, Eq. (3.6) remains valid even when the mass  $M$

is not a Schwarzschild black hole; in such a situation  $v_0$  would differ from  $6^{-1/2}$ . The same will be true for most of the equations listed below.

Next, we use Eqs. (2.6), (3.1), (3.2), and (3.5) to obtain

$$\begin{aligned} \mathcal{V} &= 3.95 \times 10^{-6} \left( \frac{p}{7.30} \right) \left( \frac{q}{1.9746} \right)^{-1} \left( \frac{\mu}{10 M_\odot} \right) \\ &\times \left( \frac{M}{10^6 M_\odot} \right)^{-1} \left( \frac{v_0}{0.4083} \right)^5 \end{aligned} \quad (3.7)$$

and

$$\alpha \simeq 1.62. \quad (3.8)$$

Continuing with our estimates, we consider a situation in which the gravitational waves are monitored during an entire year before the mass  $\mu$  reaches the innermost stable circular orbit. We ask: what is the corresponding fractional change in frequency? To answer this we integrate Eq. (2.5) for  $t(F)$ :

$$t(F) = t_0 - \frac{3}{2\pi\mathcal{V}f_0} (1 - F/f_0)^2 (1 + \dots). \quad (3.9)$$

Choosing  $f_i$  to be the initial frequency, letting  $\Delta t \equiv t_0 - t(f_i)$ ,  $\varepsilon \equiv 1 - f_i/f_0$ , and ignoring the corrections terms in Eq. (3.9), we obtain

$$\varepsilon = \left( \frac{2\pi}{3} \mathcal{V} f_0 \Delta t \right)^{1/2} \quad (3.10)$$

$$= 1.07 \left( \frac{f_0}{4.40 \text{ mHz}} \right)^{1/2} \left( \frac{\mathcal{V}}{3.95 \times 10^{-6}} \right)^{1/2} \left( \frac{\Delta t}{\text{yr}} \right)^{1/2}.$$

We recall that according to Eqs. (2.12) and (3.7), the signal must be cut off at a final frequency  $f_f$  given by

$$1 - f_f/f_0 = \mathcal{V} \sim 10^{-6}. \quad (3.11)$$

Finally, we estimate  $\mathcal{N}$ , the number of wave cycles received by the detector during the year's worth of observation. Even though the signal is not monochromatic, for our purposes it is sufficient to *define*

$$\begin{aligned} \mathcal{N} &= f_0 \Delta t \\ &= 1.39 \times 10^5 \left( \frac{f_0}{4.40 \text{ mHz}} \right) \left( \frac{\Delta t}{\text{yr}} \right) \\ &= \frac{3\varepsilon^2}{2\pi\mathcal{V}}. \end{aligned} \quad (3.12)$$

The last line follows from Eq. (3.10) and is displayed here for future reference. We see from Eq. (3.12) that for an integration time of one year, the total number of wave cycles is quite appreciable.



#### IV. KERR BLACK HOLE

We now generalize the discussion of the previous section to the case of a Kerr black hole.

As before we have that the dominant component of the gravitational waves has a frequency given by  $F = \Omega/\pi$ . For a Kerr black hole, this reads [20]

$$\pi M F = \frac{1}{r^{3/2} + \chi}. \quad (4.1)$$

Here, we use a dimensionless radial coordinate  $r$  which is a rescaled version of the usual Boyer-Lindquist coordinate, namely,  $r = r_{\text{BL}}/M$ . The dimensionless constant  $\chi$  is related to  $\mathbf{J}$ , the intrinsic (spin) angular momentum of the black hole, and also to  $\hat{\mathbf{L}}$ , the unit vector pointing in the direction of orbital angular momentum:

$$\chi = \frac{\mathbf{J} \cdot \hat{\mathbf{L}}}{M^2}. \quad (4.2)$$

Thus,  $\chi$  is *positive* if the orbital motion proceeds in the same direction as the black-hole rotation (such an orbit will be termed *direct*);  $\chi$  is *negative* if the orbital motion proceeds in the direction opposite to the black-hole rotation (such an orbit will be termed *retrograde*). It should be noted that  $\chi$  is restricted to the interval  $[-1, 1]$ ;  $|\chi| = 1$  describes an extreme Kerr black hole.

The innermost stable circular orbit is located at the value of  $r$  which satisfies  $r^2 - 6r + 8\chi r^{1/2} - 3\chi^2 = 0$ . The solution is [20]

$$\begin{aligned} \bar{r} &= 3 + B - \frac{\chi}{|\chi|} \sqrt{(3-A)(3+A+2B)}, \\ A &= 1 + (1 - \chi^2)^{1/3} \left[ (1 + \chi)^{1/3} + (1 - \chi)^{1/3} \right], \\ B &= \sqrt{3\chi^2 + A^2}. \end{aligned} \quad (4.3)$$

We observe that for  $\chi = 0$ ,  $\bar{r} = 6$ , the Schwarzschild value. For  $\chi = -1$  (extreme black hole, retrograde orbit) we have  $\bar{r} = 9$ , while  $\bar{r} = 1$  for  $\chi = 1$  (extreme black hole, direct orbits). The equation  $r = 1$  also describes the event horizon of an extreme Kerr black hole. It is useful to record the expansion

$$\begin{aligned} \bar{r} &= 1 + 2^{2/3} (1 - \chi)^{1/3} + \frac{7}{25^{1/3}} (1 - \chi)^{2/3} \\ &+ \frac{15}{16} (1 - \chi) + \dots, \end{aligned} \quad (4.4)$$

which is valid for  $\chi$  approaching unity.

Combining Eqs. (2.2) and (4.1) gives

$$\pi M f_0 \equiv v_0^3 = \frac{1}{\bar{r}^{3/2} + \chi}. \quad (4.5)$$

A plot of  $v_0^3(\chi)$  is provided in Fig. 1. We note that for  $\chi = 0$ ,  $v_0^3$  reduces to the Schwarzschild value,  $6^{-3/2} \simeq 0.0680$ . For  $\chi = -1$ ,  $v_0^3 = 1/26 \simeq 0.0385$ , while  $v_0^3 =$

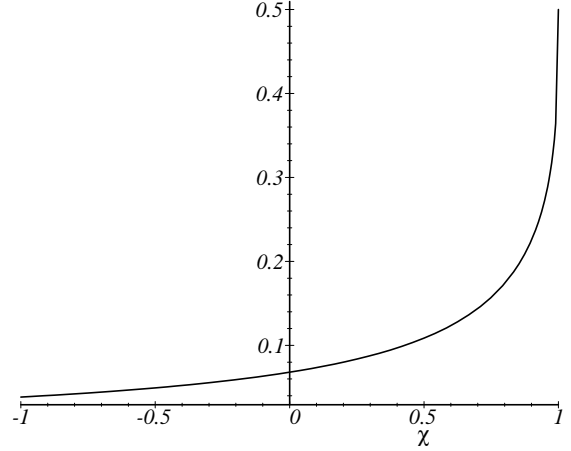


FIG. 1. A plot of  $\pi M f_0 \equiv v_0^3$  as a function of  $\chi$ .

$1/2$  for  $\chi = 1$ . We also calculate, for orbits approaching the innermost stable circular orbit,

$$\begin{aligned} 1 - F/f_0 &= \frac{r^{3/2} - \bar{r}^{3/2}}{r^{3/2} + \chi} \\ &= \frac{3\bar{r}^{1/2}}{2(\bar{r}^{3/2} + \chi)} (r - \bar{r}) \\ &\quad - \frac{3(5\bar{r}^{3/2} - \chi)}{8\bar{r}^{1/2}(\bar{r}^{3/2} + \chi)} (r - \bar{r})^2 + \dots \end{aligned} \quad (4.6)$$

This series can be inverted to give

$$\begin{aligned} r - \bar{r} &= \frac{2(\bar{r}^{3/2} + \chi)}{3\bar{r}^{1/2}} (1 - F/f_0) \\ &\quad + \frac{(5\bar{r}^{3/2} - \chi)(\bar{r}^{3/2} + \chi)}{9\bar{r}^2} (1 - F/f_0)^2 \\ &\quad + \dots \end{aligned} \quad (4.7)$$

We will use this result in order to reproduce, for the specific case of a Kerr black hole, the expansions (2.3) and (2.4) for  $dE/dt$  and  $dE/dF$ , respectively.

The computation of the gravitational-wave luminosity,  $\dot{E}_{\text{GW}} \equiv -dE/dt$ , for a specified circular orbit of the Kerr spacetime, is carried out numerically using the methods of black-hole perturbation theory [25]. In such calculations, the value of the radius is conveniently used to characterize the orbit. By computing  $\dot{E}_{\text{GW}}(\bar{r})$  and  $\dot{E}'_{\text{GW}}(\bar{r})$ , where a prime denotes differentiation with respect to  $r$ , we have access to the parameters  $p$  and  $\hat{p}$ . The precise relations are

$$p = \left( \frac{M}{\mu} \right)^2 \frac{\dot{E}_{\text{GW}}(\bar{r})}{v_0^{10}}, \quad (4.8)$$

$$\hat{p} = -\frac{2}{3\bar{r}^{1/2} v_0^3} \frac{\dot{E}'_{\text{GW}}(\bar{r})}{\dot{E}_{\text{GW}}(\bar{r})}.$$

TABLE I. The tabulated form of  $p$  and  $\hat{p}$  as functions of  $\chi$ . These values were obtained from numerical data provided by Masaru Shibata.

$\chi$	$p$	$\hat{p}$
-0.9	7.79	3.76
-0.8	7.75	3.77
-0.7	7.70	3.78
-0.6	7.65	3.78
-0.5	7.60	3.78
-0.4	7.55	3.78
-0.3	7.49	3.78
-0.2	7.43	3.78
-0.1	7.36	3.78
0.0	7.30	3.78
0.1	7.21	3.77
0.2	7.12	3.80
0.3	7.02	3.77
0.4	6.90	3.77
0.5	6.75	3.76
0.6	6.57	3.75
0.7	6.33	3.72
0.8	5.95	3.66
0.9	5.22	3.46

These parameters are listed in Table I for several values of  $\chi$ . The data from which  $p$  and  $\hat{p}$  were obtained was kindly provided by Masaru Shibata (Osaka University, Japan). Because it is increasingly difficult to calculate  $\dot{E}_{\text{GW}}$  for increasing values of  $|\chi|$ , such computations were not carried out for  $|\chi| > 0.9$ .

As for the case of a Schwarzschild black hole, the calculation of  $dE/dF$ , and its expansion near the innermost stable circular orbit, proceeds analytically.

We begin with the relation between orbital energy and radius [20]:

$$E/\mu = \frac{r^{3/2} - 2r^{1/2} + \chi}{r^{3/4}(r^{3/2} - 3r^{1/2} + 2\chi)^{1/2}}. \quad (4.9)$$

After differentiation and upon using Eq. (4.1), we obtain

$$\frac{dE}{dF} = -\frac{\pi\mu M}{3} \frac{(r^2 - 6r + 8\chi r^{1/2} - 3\chi^2)(r^{3/2} + \chi)^2}{r^{9/4}(r^{3/2} - 3r^{1/2} + 2\chi)^{3/2}}. \quad (4.10)$$

We recognize, in the numerator, the expression  $r^2 - 6r + 8\chi r^{1/2} - 3\chi^2$  which vanishes when  $r = \bar{r}$ . An expansion about this point will therefore be of the form (2.4), as we shall see presently.

We point out that this statement is *false* in the case of direct orbits around an extreme Kerr black hole. When  $\chi = 1$  the denominator of  $dE/dF$  also goes to zero at  $r = \bar{r} = 1$ , and as a consequence,  $dE/dF$  does not vanish at  $r = \bar{r}$ . Instead,

$$\lim_{r \rightarrow 1} \left( \frac{dE}{dF} \Big|_{\chi=1} \right) = -\frac{16\pi\mu M}{9\sqrt{3}}. \quad (4.11)$$

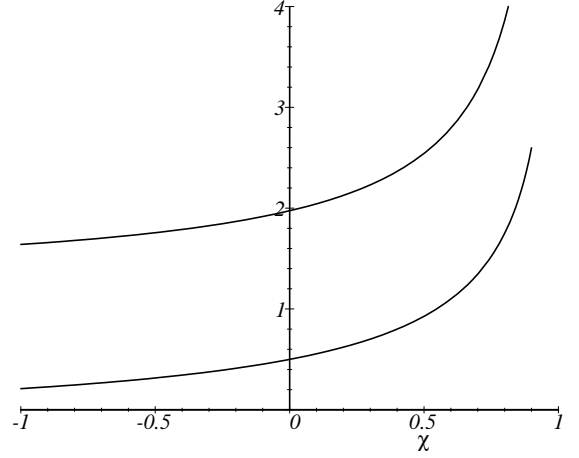


FIG. 2. Plots of  $q$  (higher curve) and  $\hat{q}$  (lower curve) as functions of  $\chi$ . Both quantities diverge as  $\chi \rightarrow 1$ .

We may therefore conclude that the condition  $r = \bar{r}$  does not, in the case of direct orbits around an extreme Kerr black hole, correspond to a genuine innermost stably circular orbit, since  $dE/dF$  fails to go to zero there. The case  $\chi = 1$  therefore represents a singular limit in the framework introduced in Sec. II, and we shall exclude it from further considerations. More details about this point can be found in the Appendix.

As was stated before, expansion of Eq. (4.10) about  $r = \bar{r}$  and substitution of Eq. (4.7) reproduces Eq. (2.4), with

$$q = \frac{4\pi}{9v_0^8 \bar{r}^{13/4} (\bar{r}^{3/2} - 3\bar{r}^{1/2} + 2\chi)^{1/2}}, \quad (4.12)$$

and

$$\hat{q} = \frac{-\bar{r}^3 + 15\bar{r}^2 + 3\chi\bar{r}^{3/2} - 39\chi\bar{r}^{1/2} + 22\chi^2}{6\bar{r}^{3/2}(\bar{r}^{3/2} - 3\bar{r}^{1/2} + 2\chi)}. \quad (4.13)$$

Plots of  $q(\chi)$  and  $\hat{q}(\chi)$  are provided in Fig. 2. We observe that for  $\chi = 0$ , Eqs. (4.12) and (4.13) reduce to the Schwarzschild expressions given by Eq. (3.5). For  $\chi = -1$ ,  $q \simeq 1.6401$  and  $\hat{q} = 17/81 \simeq 0.2100$ . For  $\chi$  approaching +1,  $q \sim (16\sqrt{12}\pi/27)(1 - \chi)^{-1/3}$  and  $\hat{q} \sim (2^{7/3}/3)(1 - \chi)^{-1/3}$ . In view of Eq. (4.11), it is not surprising that these quantities should diverge in this limit.

We use our results for  $v_0$ ,  $p$ ,  $\hat{p}$ ,  $q$ , and  $\hat{q}$  to calculate  $\mathcal{V}$  and  $\alpha$  according to Eq. (2.6). Plots of these quantities are provided in Figs. 3 and 4.

Before leaving this section we point out that Eqs. (3.6), (3.7), and (3.10)–(3.12), which provide estimates for  $f_0$ ,  $\mathcal{V}$ ,  $f_i/f_0$ ,  $f_f/f_0$ , and  $\mathcal{N}$ , are quite general: they therefore apply equally well to the case of a rotating black hole.

## V. ESTIMATION OF SIGNAL PARAMETERS

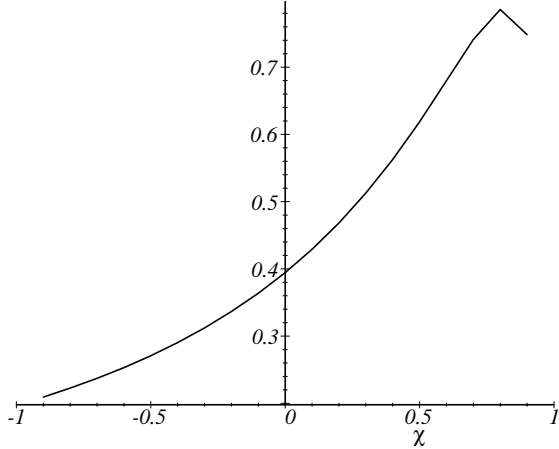


FIG. 3. A plot of  $(M/\mu)\mathcal{V}$  as a function of  $\chi$ . The computed data points at  $\chi = \{-0.9, -0.8, \dots, 0.9\}$  are joined by straight line segments.

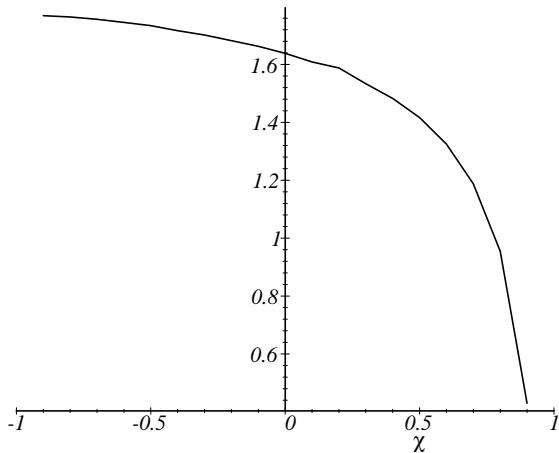


FIG. 4. A plot of  $\alpha$  as a function of  $\chi$ . The computed data points at  $\chi = \{-0.9, -0.8, \dots, 0.9\}$  are joined by straight line segments.

### A. Introduction

The last two sections were devoted to special cases of the general framework introduced in Sec. II. In such cases there exists a specific relationship between the signal parameters  $\{f_0, \mathcal{V}, \alpha\}$  and the source parameters  $\{\mu, M, \chi\}$ . For example, in the case of a Kerr black hole,  $\alpha$  is a function of the single variable  $\chi$ ; this function is represented in Fig. 4.

We now return to the general framework of Sec. II, in which the nature of the mass  $M$  is left unspecified. The framework also makes no specific choice regarding the correct description of gravitational radiation.

In this framework the gravitational-wave signal is given by Eq. (2.10), which we rewrite as

$$\tilde{h}(f) = \mathcal{A} (1 - f/f_0)^{1/2} e^{i\psi(f)},$$

$$\psi(f) = 2\pi f t_0 - \phi_0 + \phi(f), \quad (5.1)$$

$$\phi(f) = \frac{(1 - f/f_0)^3}{\mathcal{V}} [1 + \alpha(1 - f/f_0)].$$

For the purpose of this section we consider Eq. (5.1) to be exact, ignoring all relative corrections of order  $(1 - f/f_0)$  in the amplitude, and all relative corrections of order  $(1 - f/f_0)^2$  in the phase.

The signal is characterized by six parameters, which we group into the vector

$$\boldsymbol{\theta} = (\ln \mathcal{A}, \ln f_0, \ln \mathcal{V}, \alpha, t_0, \phi_0). \quad (5.2)$$

The purpose of this section is to calculate, for a given signal strength, how accurately the parameters  $\boldsymbol{\theta}$  can be estimated during a gravitational-wave measurement.

### B. Parameter estimation

The statistical theory of signal detection and measurement [33,34] has repeatedly been applied to the specific case of gravitational waves [35,36]. For a complete exposition, we refer the reader to Refs. [15,18,37]. That the theory must be statistical in character follows from the facts that gravitational-wave detectors are noisy, and that the noise is a random process, here assumed to be stationary and Gaussian. In this subsection we apply the theory to calculate, in the limit of large signal-to-noise ratio, the expected statistical errors associated with the estimation of the signal parameters  $\boldsymbol{\theta}$ .

We first introduce the inner product  $(\cdot|\cdot)$ : If  $a$  and  $b$  are two functions of time, with Fourier transforms  $\tilde{a}$  and  $\tilde{b}$ , then

$$(a|b) = 2 \int_0^\infty \frac{\tilde{a}^*(f) \tilde{b}(f) + \tilde{a}(f) \tilde{b}^*(f)}{S_n(f)} df. \quad (5.3)$$

Here, an asterisk denotes complex conjugation, and  $S_n(f)$  is the spectral density of the detector noise, the Fourier transform of the noise's autocorrelation function. The detector has good sensitivity where  $S_n(f)$  is small, and poor sensitivity where  $S_n(f)$  is large. For LISA,  $S_n(f)$  is small in the frequency bandwidth between  $10^{-4}$  and  $10^{-1}$  Hz [1]. The precise behavior, and overall normalization, of  $S_n(f)$  will be of no concern to us.

The *signal-to-noise ratio*  $\rho$  associated with the measurement of a signal  $h(t)$  by a detector with spectral density  $S_n(f)$  is given by  $\rho^2 = (h|h)$ . This is simply evaluated for our model signal (5.1). Expanding the spectral density as  $S_n(f) = S_n(f_0)[1 + O(1 - f/f_0)]$ , neglecting the second term for consistency, and integrating from  $f = f_i$  to  $f = f_f$ , we obtain

$$\rho^2 = \frac{2f_0 |\mathcal{A}|^2 \varepsilon^2}{S_n(f_0)}. \quad (5.4)$$

Here,  $\varepsilon = 1 - f_i/f_0$ , and is given by Eq. (3.10). We have neglected  $\mathcal{V}^2$  in front of  $\varepsilon^2$ , cf. Eq. (3.11). From Eq. (5.4)

we see that the signal-to-noise ratio is proportional to the signal's amplitude times the square root of its duration (as measured by  $\varepsilon$ ), and inversely proportional to the noise's amplitude.

We calculate the anticipated accuracy with which the parameters  $\theta$  can be estimated during a gravitational-wave measurement. In the limit of large signal-to-noise ratio (or small statistical errors), the calculation involves computing, and then inverting, the Fisher information matrix  $\Gamma_{ab} = (h_{,a}|h_{,b})$ , where  $h_{,a} = \partial h / \partial \theta^a$  is the partial derivative of the signal with respect to the parameter  $\theta^a$ .

With the ordering provided by Eq. (5.2), the partial derivatives are given by

$$\tilde{h}_{,a} = g_a \tilde{h}, \quad (5.5)$$

where

$$\begin{aligned} g_1 &= 1, \\ g_2 &= \frac{1-x}{2x} \left[ 1 + \frac{2ix^3}{\mathcal{V}} (3 + 4\alpha x) \right], \\ g_3 &= -\frac{ix^3}{\mathcal{V}} (1 + \alpha x), \\ g_4 &= \frac{ix^4}{\mathcal{V}}, \\ g_5 &= i(2\pi f_0)(1-x), \\ g_6 &= -i, \end{aligned} \quad (5.6)$$

and  $x = 1 - f/f_0$ . Then, using Eq. (5.4) and the same approximation for  $S_n(f)$  as was used before, we have that

$$\Gamma_{ab} = \frac{\rho^2}{\varepsilon^2} \int_{\mathcal{V}} [g_a^*(x) g_b(x) + g_a(x) g_b^*(x)] x dx. \quad (5.7)$$

These integrations are easily carried out. Because its expression is rather large, the Fisher matrix will not be displayed here.

The meaning of the Fisher matrix is as follows [15,18]. Because of random noise, the output of a gravitational-wave detector is also random, even when a signal of the form  $h(t; \theta)$  is known to be present. Consequently, an estimation of the parameters  $\theta$  comes with inevitable statistical uncertainty. It can be shown that in the limit of large signal-to-noise ratio, the probability distribution function for the parameters  $\theta$  is of the Gaussian form  $\exp[-\frac{1}{2}\Gamma_{ab}(\theta^a - \bar{\theta}^a)(\theta^b - \bar{\theta}^b)]$ , where  $\bar{\theta}$  denotes the true value of the signal parameters. It follows that the variance-covariance matrix,  $\Sigma^{ab} \equiv \langle (\theta^a - \bar{\theta}^a)(\theta^b - \bar{\theta}^b) \rangle$ , where  $\langle \cdot \rangle$  denotes an averaging with respect to the specified distribution, is given simply by the inverse of the Fisher matrix,

$$\Sigma^{ab} = (\Gamma^{-1})^{ab}. \quad (5.8)$$

In terms of this, the ‘‘one-sigma’’ statistical error associated with the estimation of parameter  $\theta^a$  is given by

$$\Delta\theta^a = \sqrt{\Sigma^{aa}}, \quad (5.9)$$

where there is no summation over the repeated indices.

To invert the Fisher matrix we proceed as follows. After computing the matrix we use Eq. (3.12) to express  $\mathcal{V}$  in terms of  $\varepsilon$  and  $\mathcal{N}$ . The matrix is then inverted algebraically, using the symbolic manipulator Maple. Thus far all expressions are exact, and quite large. To simplify, we take advantage of the fact that according to Eq. (3.12),  $\mathcal{N}$  is numerically very large. We therefore expand our exact expression for  $\Sigma$  in powers of  $1/\mathcal{N}$ , keeping only the leading-order term. It can be verified that the resulting matrix is equal to ***Sigma***, apart from a fractional correction of order  $1/\mathcal{N}^2$ .

We obtain the following results:

$$\begin{aligned} \frac{\Delta\mathcal{A}}{\mathcal{A}} &= \frac{1}{\rho}, \\ \frac{\Delta f_0}{f_0} &= \frac{280\sqrt{3}}{2\pi\mathcal{N}\rho}, \\ \frac{\Delta\mathcal{V}}{\mathcal{V}} &= \frac{1890\sqrt{a}}{2\pi\mathcal{N}\varepsilon\rho}, \\ \Delta\alpha &= \frac{378\sqrt{5b}}{2\pi\mathcal{N}\varepsilon^2\rho}, \\ \Delta t_0 &= \frac{105\sqrt{2}}{2\pi f_0\varepsilon\rho}, \\ \Delta\phi_0 &= \frac{105\sqrt{2c}}{\varepsilon\rho}, \end{aligned} \quad (5.10)$$

where

$$\begin{aligned} a(\varepsilon, \alpha) &= 1 - \left( \frac{32}{21} - \frac{128}{63}\alpha \right) \varepsilon \\ &\quad + \left( \frac{16}{27} - \frac{128}{81}\alpha + \frac{256}{243}\alpha^2 \right) \varepsilon^2, \\ b(\varepsilon, \alpha) &= 1 + \frac{40}{9}\alpha\varepsilon + \frac{5}{9}(2 + 17\alpha)\alpha\varepsilon^2 \\ &\quad + \frac{160}{63}(1 + 4\alpha)\alpha^2\varepsilon^3 + \frac{80}{243}(1 + 4\alpha)^2\alpha^2\varepsilon^4, \\ c(\varepsilon) &= 1 - \frac{4}{21}\varepsilon + \frac{1}{98}\varepsilon^2. \end{aligned} \quad (5.11)$$

To put this in a more concrete form we evaluate  $a$ ,  $b$ , and  $c$  at  $\varepsilon = 1.1$  and  $\alpha = 1.6$ ; cf. Eqs. (3.8) and (3.10). This gives  $a \simeq 3.8$ ,  $b \simeq 170$ , and  $c \simeq 0.80$ . We then choose  $\mathcal{N} = 1.4 \times 10^5$  and  $f_0 = 4.4$  mHz as fiducial values. Substituting all this, we obtain

$$\begin{aligned} \frac{\Delta\mathcal{A}}{\mathcal{A}} &= \frac{1}{\rho}, \\ \frac{\Delta f_0}{f_0} &\simeq \frac{5.5 \times 10^{-4}}{\rho} \left( \frac{\mathcal{N}}{1.4 \times 10^5} \right)^{-1}, \\ \frac{\Delta\mathcal{V}}{\mathcal{V}} &\simeq \frac{3.8 \times 10^{-3}}{\rho} \left( \frac{a}{3.8} \right)^{1/2} \left( \frac{\varepsilon}{1.1} \right)^{-1} \left( \frac{\mathcal{N}}{1.4 \times 10^5} \right)^{-1}, \\ \Delta\alpha &\simeq \frac{1.0 \times 10^{-2}}{\rho} \left( \frac{b}{170} \right)^{1/2} \left( \frac{\varepsilon}{1.1} \right)^{-2} \left( \frac{\mathcal{N}}{1.4 \times 10^5} \right)^{-1}, \end{aligned}$$

$$\begin{aligned}\Delta t_0 &\simeq \frac{81 \text{ min}}{\rho} \left( \frac{f_0}{4.4 \text{ mHz}} \right)^{-1} \left( \frac{\varepsilon}{1.1} \right)^{-1}, \\ \Delta \phi_0 &\simeq \frac{19 \text{ cycles}}{\rho} \left( \frac{c}{0.80} \right)^{1/2} \left( \frac{\varepsilon}{1.1} \right)^{-1}.\end{aligned}\quad (5.12)$$

From these expressions we observe that: (i) The relative accuracy with which  $\mathcal{A}$ , the amplitude parameter, can be estimated is precisely equal to the inverse signal-to-noise ratio. We shall call this level of accuracy the “signal-to-noise ratio level”. (ii) The estimation of  $f_0$  benefits the most from the large number of wave cycles; its accuracy is typically three orders of magnitude better than the signal-to-noise ratio level. (iii) The estimation of  $\mathcal{V}$  and  $\alpha$  also benefits from the large value of  $\mathcal{N}$ ; their accuracies are respectively three and two orders of magnitude better than the signal-to-noise ratio level. (iv) The uncertainties associated with the parameters  $t_0$  and  $\phi_0$  are independent of  $\mathcal{N}$ .

### C. Measurement of black-hole parameters

For the purpose of this subsection we return to the special case in which the mass  $M$  is a Kerr black hole (Sec. IV). The question we ask is: What does a measurement of the signal parameters  $\{f_0, \mathcal{V}, \alpha\}$  tell us about the source parameters  $\{\mu, M, \chi\}$ ?

Inspection of Figs. 1, 3, and 4 reveals that the quantities  $\pi M f_0 \equiv v_0^3$ ,  $\eta^{-1} \mathcal{V}$ , and  $\alpha$  are all functions of the single variable  $\chi$ . Here we have defined  $\eta$  to be the mass ratio:

$$\eta = \frac{\mu}{M}. \quad (5.13)$$

We therefore write

$$\begin{aligned}\pi M f_0 &= A(\chi), \\ \eta^{-1} \mathcal{V} &= B(\chi), \\ \alpha &= C(\chi).\end{aligned}\quad (5.14)$$

It follows from these relations that a measurement of  $\alpha$  yields the value of  $\chi$ . Knowing  $\chi$ , a measurement of  $\mathcal{V}$  then gives  $\eta$ . And finally, a measurement of  $f_0$  returns the value of  $M$ . In this way, the source parameters can all be estimated from a measurement of the gravitational-wave signal. The question remains as to how accurately all this can be done. This is the question we turn to next.

We first consider the estimation of  $\chi$ , the black-hole rotation parameter. It follows from Eq. (5.14) that in the limit of small measurement uncertainties, the error in  $\chi$  is given by

$$\Delta \chi = \frac{1}{|C'(\chi)|} \Delta \alpha, \quad (5.15)$$

where a prime denotes differentiation with respect to  $\chi$ . To express this in a more concrete form it would be desirable to explicitly compute the function  $C'(\chi)$ . Unfortunately, this cannot be done reliably, since  $C(\chi)$  was

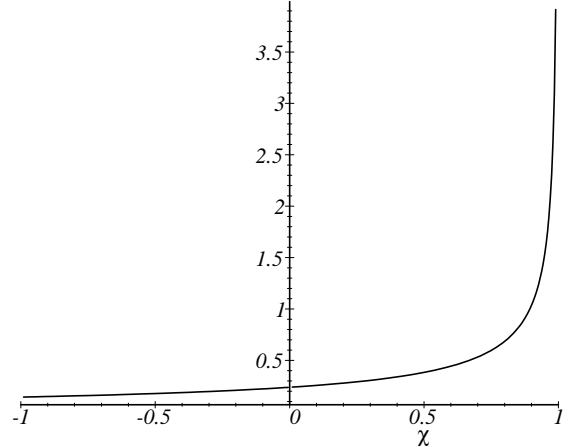


FIG. 5. A plot of  $A'/\pi A$  as a function of  $\chi$ .

evaluated at only a few widely separated points. Nevertheless, we crudely estimate  $C'(\chi)$  to be 0.2 at the somewhat representative point  $\chi = 0$ . This yields

$$\Delta \chi \simeq 5.0 \Delta \alpha \quad \text{for } \chi = 0. \quad (5.16)$$

It can be seen from Fig. 4 that the uncertainty in  $\chi$  would be larger than this for negative values of  $\chi$ , while it would be smaller (and going to zero for  $\chi \rightarrow 1$ ) for positive values. Using Eq. (5.12), Eq. (5.16) means that for typical situations,  $\Delta \chi \simeq 5.0 \times 10^{-2}/\rho$ . The rotation parameter can therefore be estimated with a degree of accuracy approximately two orders of magnitude better than the signal-to-noise ratio level.

We now repeat this procedure for  $\eta$ , the mass-ratio parameter. In the limit of small uncertainties, Eq. (5.14) implies

$$\frac{\Delta \eta}{\eta} = \left| \frac{B'(\chi)}{B(\chi)} \right| \Delta \chi + \frac{\Delta \mathcal{V}}{\mathcal{V}}. \quad (5.17)$$

A crude estimate reveals that  $|B'/B| \simeq 1.1$  at  $\chi = 0$ . This means that the uncertainty in  $\chi$  dominates the uncertainty in  $\eta$ , and we find

$$\frac{\Delta \eta}{\eta} \simeq 1.1 \Delta \chi \quad \text{for } \chi = 0. \quad (5.18)$$

For typical situations,  $\Delta \eta/\eta \simeq 5.5 \times 10^{-2}/\rho$ , a degree of accuracy one order of magnitude better than the signal-to-noise ratio level.

Finally, we consider the accuracy with which  $M$ , the black-hole mass, can be estimated. We once more use Eq. (5.14) to derive

$$\pi \frac{\Delta M}{M} = \left| \frac{A'(\chi)}{A(\chi)} \right| \Delta \chi + \frac{\Delta f_0}{f_0}. \quad (5.19)$$

A plot of  $A'/\pi A$  is provided in Fig. 5. Once more we find that the uncertainty in  $\chi$  dominates over the other contribution. Evaluation at  $\chi = 0$  yields

$$\frac{\Delta M}{M} \simeq 0.238\Delta\chi \quad \text{for } \chi = 0. \quad (5.20)$$

It can be seen from Fig. 5 that the uncertainty in  $M$  would be smaller than this for negative values of  $\chi$ , larger for positive values, and significantly larger for  $\chi$  approaching unity. For typical situations,  $\Delta M/M \simeq 2.4 \times 10^{-3}/\rho$ , a degree of accuracy three orders of magnitude better than the signal-to-noise ratio level.

The bottom line is that during a gravitational-wave measurement, the source parameters  $\{\mu, M, \chi\}$  can be estimated with a degree of accuracy that is much better than the signal-to-noise ratio level.

#### D. Testing general relativity

Since the framework of Sec. II makes no explicit reference to a particular model for the mass  $M$ , nor to a particular theory of gravitation, we may ask whether it leads to a viable strategy for testing the strong-field predictions of general relativity. More precisely, we ask: Can a measurement of the signal parameters  $\{f_0, \mathcal{V}, \alpha\}$  allow us to test the hypothesis according to which the central object is a Kerr black hole and the correct theory of gravitation is general relativity?

Clearly, measuring  $f_0$  and  $\mathcal{V}$  if of no use in this purpose. This is because  $f_0$  and  $\mathcal{V}$  respectively depend on  $M$  and  $\eta = \mu/M$ , which are not known prior to the measurement. Therefore, measuring  $f_0$  and  $\mathcal{V}$  offers no way of distinguishing two different models for the source which, by adjusting the values of  $M$  and  $\mu$ , give identical values for  $f_0$  and  $\mathcal{V}$ .

The parameter  $\alpha$  is more useful. It is a consequence of the standard model (the mass  $M$  is a Kerr black hole and the correct theory of gravitation is general relativity) that  $\alpha$  is restricted to the interval  $I_{\text{sm}} = (-\infty, 1.8)$ . Measuring  $\alpha$  therefore leads to a way of testing general relativity, since a measured value of  $\alpha$  outside  $I_{\text{sm}}$  would unambiguously invalidate the standard model.

Of course, while viable in principle, this test is very much a partial one, and leaves much to be desired. For example, it is impossible to say which aspect of the standard model is violated when  $\alpha \notin I_{\text{sm}}$ . Another shortcoming is that there could well exist a wide class of alternative models for which  $\alpha$  is restricted to an interval  $I$  which is a *subset* of  $I_{\text{sm}}$ . The test offers no way of ruling out models belonging to this class. Finally, we must also recall that the entire framework is based upon a rather restrictive assumption: that the orbit must be circular and within the equatorial plane.

#### ACKNOWLEDGMENTS

I am most grateful to Clifford Will for his constant encouragement during the realization of this work, which originated during discussions with him. This paper could

not have been written without the kind help of Masaru Shibata, who provided the numerical data used to construct Table I. A conversation with Kip Thorne was also greatly appreciated. This work was supported by the Natural Sciences and Engineering Research Council of Canada, by the National Science Foundation under Grant No. PHY 92-22902, and by the National Aeronautics and Space Administration under Grant No. NAGW 3874.

#### APPENDIX:

In this Appendix we consider the motion of a test mass in a spacetime satisfying the following properties: it is stationary and asymptotically flat, possesses axial symmetry, and is reflection symmetric about the equatorial plane. We do not assume that the spacetime metric satisfies the Einstein field equations. However, for simplicity we shall assume that the test mass is moving freely, so that it follows a geodesic of the spacetime. Generalization to the presence of external forces (which also satisfy the symmetry requirements) would be straightforward. We shall focus our attention on equatorial, circular orbits, the meaning of which will be made precise below.

The results obtained in this Appendix form the basis for the construction of the model signal of Sec. II.

#### 1. Equations of motion

We introduce coordinates  $(t, r, \theta, \phi)$  to chart the spacetime. We take  $t$  to be the time coordinate associated with the timelike Killing vector  $\xi = \partial/\partial t$ , and normalized such that it is equal to proper time for observers at rest at infinity. We take  $r$  to be a well-behaved radial coordinate, such that circular orbits (defined in a coordinate-invariant way below) are described by  $r = \text{constant}$ . We take  $\theta$  and  $\phi$  to be the usual spherical coordinates, such that  $\phi$  is associated with the Killing vector  $\chi = \partial/\partial\phi$ . In these coordinates, according to the specified symmetries, the only off-diagonal component of the metric is  $g_{t\phi}$ . For the specific case of a Kerr black hole, the coordinates employed reduce to the Boyer-Lindquist coordinates [19].

Reflection symmetry about the equatorial plane ensures that the motion of a test mass can be restricted to lie in this plane. (Of course, such a restriction represents a loss of generality). We therefore take  $\theta = \pi/2$ , and the four-velocity is  $u^\alpha = dx^\alpha/d\tau = (\dot{t}, \dot{r}, 0, \dot{\phi})$ , where an overdot denotes differentiation with respect to proper time  $\tau$ . The quantities

$$\tilde{E} = -\mathbf{u} \cdot \boldsymbol{\xi}, \quad \tilde{L} = \mathbf{u} \cdot \boldsymbol{\chi} \quad (A1)$$

are constants of the motion, respectively representing orbital energy per unit rest mass, and orbital angular momentum per unit rest mass.

It is easy to show that Eqs. (A1) imply

$$\dot{t} = T(r, \tilde{E}, \tilde{L}) \equiv (g_{\phi\phi}\tilde{E} + g_{t\phi}\tilde{L})/D, \quad (\text{A2})$$

$$\dot{\phi} = \Phi(r, \tilde{E}, \tilde{L}) \equiv -(g_{t\phi}\tilde{E} + g_{tt}\tilde{L})/D,$$

where  $D = -g_{tt}g_{\phi\phi} + g_{t\phi}^2$ . On the other hand, the normalization condition  $\mathbf{u} \cdot \mathbf{u} = -1$  gives

$$\dot{r}^2 = R(r, \tilde{E}, \tilde{L}) = -\frac{1}{g_{rr}} + \frac{g_{\phi\phi}\tilde{E}^2 + 2g_{t\phi}\tilde{E}\tilde{L} + g_{tt}\tilde{L}^2}{g_{rr}D}. \quad (\text{A3})$$

As was indicated, the metric functions are considered to be functions of  $r$  only, since they are evaluated at  $\theta = \pi/2$ .

We define a function  $\Omega$  by

$$\Omega(r, \tilde{E}, \tilde{L}) = \frac{d\phi}{dt} = \frac{\Phi(r, \tilde{E}, \tilde{L})}{T(r, \tilde{E}, \tilde{L})}. \quad (\text{A4})$$

This represents the angular velocity of the test mass, as measured by an observer at rest at infinity.

## 2. Circular orbits

We define an orbit to be circular if  $r$  is constant along the orbit. The conditions for this to be true are  $\dot{r} = \ddot{r} = 0$ . According to Eq. (A3), this means

$$R(r, \tilde{E}, \tilde{L}) = \frac{\partial R}{\partial r}(r, \tilde{E}, \tilde{L}) = 0. \quad (\text{A5})$$

These equations determine the values that  $\tilde{E}$  and  $\tilde{L}$  must take in order to produce a circular orbit at radius  $r$ . For an orbit at  $r = r_0$ , we shall denote these values by  $\tilde{E}_0$  and  $\tilde{L}_0$ .

Let  $\Omega_0$  be the angular-velocity function evaluated at  $r = r_0$ ,  $\tilde{E} = \tilde{E}_0(r_0)$ , and  $\tilde{L} = \tilde{L}_0(r_0)$ . We therefore have the important result that the angular velocity is uniform along a circular orbit. This provides a coordinate-invariant definition of circularity, a property that has nothing to do with the geometric appearance of the orbit. As a condition on our choice of radial coordinate, we require that  $\Omega_0$  be a smooth, monotonic function of  $r_0$ .

## 3. Neighboring circular orbits

We now consider two neighboring circular orbits, the first at  $r = r_0$  (with associated parameters  $\tilde{E}_0$  and  $\tilde{L}_0$ ), the second at  $r = r_1$  (with associated parameters  $\tilde{E}_1$  and  $\tilde{L}_1$ ). We assume that  $r_1 = r_0 + \delta r_0$ , with  $\delta r_0$  a small quantity. Correspondingly,  $\tilde{E}_1 = \tilde{E}_0 + \delta\tilde{E}_0$  and  $\tilde{L}_1 = \tilde{L}_0 + \delta\tilde{L}_0$ . We want to calculate various relationships between the displacements  $\delta r_0$ ,  $\delta\tilde{E}_0$ , and  $\delta\tilde{L}_0$ .

From Eq. (A5) we must have  $R(r_1, \tilde{E}_1, \tilde{L}_1) = 0$ . Expanding this about  $(r_0, \tilde{E}_0, \tilde{L}_0)$ , up to first order in the displacements, gives

$$\left. \frac{\partial R}{\partial \tilde{E}} \right|_0 \delta\tilde{E}_0 + \left. \frac{\partial R}{\partial \tilde{L}} \right|_0 \delta\tilde{L}_0 = 0.$$

This equation takes a more familiar form if we use Eq. (A3) to evaluate the partial derivatives. We quickly arrive at

$$\delta\tilde{E}_0 = \Omega_0 \delta\tilde{L}_0. \quad (\text{A6})$$

Equation (A5) also implies that  $\partial_r R(r_1, \tilde{E}_1, \tilde{L}_1) = 0$ . Expanding, using Eq. (A3) to evaluate the partial derivatives, and Eqs. (A4) and (A6) to simplify the result, we arrive at

$$\left. \frac{\partial^2 R}{\partial r^2} \right|_0 \delta r_0 = \frac{2}{\Omega_0 g_{rr}} \left( \frac{\partial \Phi}{\partial r} - \Omega_0 \frac{\partial T}{\partial r} \right) \Big|_0 \delta\tilde{E}_0. \quad (\text{A7})$$

We notice that  $(\partial_r \Phi - \Omega \partial_r T)/T = \partial_r \Omega$ . Regularity of the radial coordinate therefore implies that the right-hand side of Eq. (A7) is nonzero whenever  $T \neq 0$ , or  $g_{rr} \neq \infty$ .

A similar calculation would yield  $\delta\Omega_0$  in terms of either one of  $\delta r_0$ ,  $\delta\tilde{E}_0$ , or  $\delta\tilde{L}_0$ .

## 4. Innermost stable circular orbit

We assume that the spacetime is such that stable circular orbits can only exist at radii larger than some limiting value  $r_{\text{isco}}$ . At  $r = r_{\text{isco}}$ , circular orbits become unstable, in the following sense: an infinitesimal change in the orbital energy (or orbital angular momentum) produces a finite change in the orbital radius. The innermost stable circular orbit is therefore defined to be that particular circular orbit at which

$$\left. \frac{\delta\tilde{E}_0}{\delta r_0} \right|_{\text{isco}} = 0. \quad (\text{A8})$$

We shall assume that the condition

$$\left. \frac{2}{\Omega_0 g_{rr}} \left( \frac{\partial \Phi}{\partial r} - \Omega_0 \frac{\partial T}{\partial r} \right) \right|_{\text{isco}} \neq 0 \quad (\text{A9})$$

holds. [For the specific case of a non-extreme Kerr black hole, this condition can be shown to hold for both direct and retrograde orbits, for any value of the hole's angular momentum. However, for the special case of an *extreme* Kerr black hole, the condition is violated for direct orbits. This is because  $g_{rr}|_{\text{isco}} = \infty$ , which signals the presence of an event horizon at  $r = r_{\text{isco}}$ . As a result,  $\delta\tilde{E}/\delta r_0$  never goes to zero for direct circular orbits around an extreme Kerr black hole.]

Combining Eqs. (A8) and (A9), we obtain

$$\left. \frac{\partial^2 R}{\partial r^2} \right|_{\text{isco}} = 0. \quad (\text{A10})$$

The innermost stable circular orbit corresponds to an inflection point of the effective potential  $R$ .

We have required that  $\Omega_0$  be a smooth, monotonic function of  $r_0$ . Equation (A8) therefore also implies that

$$\left. \frac{\delta \tilde{E}_0}{\delta \Omega_0} \right|_{\text{isco}} = 0. \quad (\text{A11})$$

This is a coordinate-invariant characterization of the innermost stable circular orbit.

It is easy to check that near  $r_0 = r_{\text{isco}}$ ,  $\delta \tilde{E}_0 / \delta \Omega_0 \propto \partial^2 R / \partial r^2|_0$ . We assume that  $\partial^3 R / \partial r^3$  does not vanish at  $r_0 = r_{\text{isco}}$ , so that the right-hand side vanishes linearly with  $r_0 - r_{\text{isco}}$ . We then quickly arrive at the following estimate:

$$\frac{\delta \tilde{E}_0}{\delta \Omega_0} \sim k(\Omega_0 - \Omega_{\text{isco}}), \quad (\text{A12})$$

for some constant  $k$ . This result provides the justification for Eq. (2.4), above.

---

\* E-mail address: poisson@terra.physics.uoguelph.ca.

† Permanent address.

- [1] P. Bender, I. Ciufolini, K. Danzmann, W. Folkner, J. Hough, D. Robertson, A. Rüdiger, M. Sandford, R. Schilling, B. Schutz, R. Stebbins, T. Summer, P. Touboul, S. Vitale, H. Ward, and W. Winkler, *LISA: Laser Interferometer Space Antenna for the detection and observation of gravitational waves*, Pre-Phase S Report, December 1995 (unpublished).
- [2] A. Abramovici, W.E. Althouse, R.W.P. Drever, Y. Gürsel, S. Kawamura, F.J. Raab, D. Shoemaker, L. Siewers, R.E. Spero, K.S. Thorne, R.E. Vogt, R. Weiss, S.E. Whitcomb, and M.E. Zucker, *Science* **256**, 325 (1992).
- [3] C. Cutler and L. Lindblom, *Gravitational helioseismology?*, Phys. Rev. D (to be published).
- [4] D. Hills, P.L. Bender, and R.F. Webbink, *Astrophys. J.* **360**, 75 (1990).
- [5] R.R. Caldwell and B. Allen, *Phys. Rev. D* **45**, 3447 (1992).
- [6] D. Hils and P.L. Bender, *Astrophys. J.* **445**, L7 (1995).
- [7] M. Shibata, *Phys. Rev. D* **50**, 6297 (1994).
- [8] T. Tanaka, M. Shibata, M. Sasaki, H. Tagashi, and T. Nakamura, *Prog. Theor. Phys.* **90**, 65 (1993).
- [9] C. Cutler, D. Kennefick, and E. Poisson, *Phys. Rev. D* **50**, 3816 (1994).
- [10] D. Hils and P.L. Bender (unpublished).
- [11] F.D. Ryan, *Phys. Rev. D* **52**, 5707 (1995).
- [12] L.S. Finn, A. Ori, and K.S. Thorne (unpublished).
- [13] E. Poisson, *Phys. Rev. D* **47**, 1497 (1993).
- [14] F. Echeverria, *Phys. Rev. D* **40**, 3194 (1989).
- [15] L.S. Finn, *Phys. Rev. D* **46**, 5236 (1992).
- [16] S. Chandrasekhar and S.L. Detweiler, *Proc. R. Soc. London* **A344**, 441 (1975).
- [17] L.S. Finn and D.F. Chernoff *Phys. Rev. D* **47**, 2198 (1993).
- [18] C. Cutler and É.E. Flanagan, *Phys. Rev. D* **49**, 2658 (1994).
- [19] See, for example, C.W. Misner, K.S. Thorne, and J.A. Wheeler, *Gravitation* (Freeman, San Francisco, 1973), Chapters 25 and 33.
- [20] J.M. Bardeen, W.H. Press, and S.A. Teukolsky, *Astrophys. J.* **178**, 347 (1972).
- [21] M. Shibata, M. Sasaki, H. Tagoshi, and T. Tanaka, *Phys. Rev. D* **51**, 1646 (1995).
- [22] F.D. Ryan, *Phys. Rev. D* **52**, R3159 (1995).
- [23] A. Ori, *Phys. Lett. A* **202**, 347 (1995).
- [24] For an overview, see C.M. Will, in *Relativistic Cosmology*, Proceedings of the Eighth Nishinomiya-Yukawa Memorial Symposium, edited by M. Sasaki (Universal Academy Press, Kyoto, Japan, 1994).
- [25] M. Shibata, *Phys. Rev. D* **48**, 663 (1993); *Prog. Theor. Phys.* **90**, 595 (1993).
- [26] C. Brans and R.H. Dicke, *Phys. Rev.* **124**, 925 (1961).
- [27] C.M. Will, *Phys. Rev. D* **50**, 6058 (1994).
- [28] S.W. Hawking, *Commun. Math. Phys.* **25**, 167 (1972).
- [29] See, for example, J.D. Jackson, *Classical Electrodynamics*, (Wiley, New York, 1975), p. 316.
- [30] C. Cutler, L.S. Finn, E. Poisson, and G.J. Sussman, *Phys. Rev. D* **47**, 1511 (1993).
- [31] H. Tagoshi and T. Nakamura, *Phys. Rev. D* **49** 4016 (1994).
- [32] E. Poisson, *Phys. Rev. D* **52**, 5719 (1995).
- [33] C.W. Helstrom, *Statistical Theory of Signal Detection*, (Pergamon, Oxford, England, 1968).
- [34] L.A. Wainstein and V.D. Zubakov, *Extraction of Signals from Noise*, (Prentice-Hall, Englewood Cliffs, 1962).
- [35] K.S. Thorne, in *300 Years of Gravitation*, edited by S.W. Hawking and W. Israel (Cambridge University Press, Cambridge, England, 1987).
- [36] B.F. Schutz, in *The detection of gravitational waves*, edited by D.G. Blair (Cambridge University Press, Cambridge, England, 1991).
- [37] E. Poisson and C.M. Will, *Phys. Rev. D* **52**, 848 (1995).